

# PROCEEDINGS OF SPIE

[SPIDigitalLibrary.org/conference-proceedings-of-spie](https://spiedigitallibrary.org/conference-proceedings-of-spie)

## Graph search: active appearance model based automated segmentation of retinal layers for optic nerve head centered OCT images

Enting Gao, Fei Shi, Weifang Zhu, Chao Jin, Min Sun, et al.

Enting Gao, Fei Shi, Weifang Zhu, Chao Jin, Min Sun, Haoyu Chen, Xinjian Chen, "Graph search: active appearance model based automated segmentation of retinal layers for optic nerve head centered OCT images," Proc. SPIE 10133, Medical Imaging 2017: Image Processing, 101331Q (24 February 2017); doi: 10.1117/12.2250168

**SPIE.**

Event: SPIE Medical Imaging, 2017, Orlando, Florida, United States

# Graph Search – Active Appearance Model based Automated Segmentation of Retinal Layers for Optic Nerve Head Centered OCT Images

Enting Gao<sup>1,2</sup>, Fei Shi<sup>1</sup>, Weifang Zhu<sup>1</sup>, Chao Jin<sup>1</sup>, Min Sun<sup>1</sup>, Haoyu Chen<sup>3</sup>, Xinjian Chen<sup>1\*</sup>

<sup>1</sup>School of Electronics and Information Engineering, Soochow University, Suzhou, Jiangsu Province, China

<sup>2</sup>School of Electronic and Information Engineering, Suzhou University of Science and Technology, Suzhou, China

<sup>3</sup>Joint Shantou International Eye Center, Shantou University and the Chinese University of Hong Kong, Shantou, China

## ABSTRACT

In this paper, a novel approach combining the active appearance model (AAM) and graph search is proposed to segment retinal layers for optic nerve head (ONH) centered optical coherence tomography (OCT) images. The method includes two parts: preprocessing and layer segmentation. During the preprocessing phase, images are first filtered for denoising, then the B-scans are flattened. During layer segmentation, the AAM is first used to obtain the coarse segmentation results. Then a multi-resolution GS-AAM algorithm is applied to further refine the results, in which AAM is efficiently integrated into the graph search segmentation process. The proposed method was tested on a dataset which contained 113-D SD-OCT images, and compared to the manual tracings of two observers on all the volumetric scans. The overall mean border positioning error for layer segmentation was found to be  $7.09 \pm 6.18 \mu\text{m}$  for normal subjects. It was comparable to the results of traditional graph search method ( $8.03 \pm 10.47 \mu\text{m}$ ) and mean inter-observer variability ( $6.35 \pm 6.93 \mu\text{m}$ ). The preliminary results demonstrated the feasibility and efficiency of the proposed method.

**KEYWORDS:** automated 3-D segmentation, Optical coherence tomography (OCT), retinal layers, Active Appearance Models (AAM), graph search

## 1. INTRODUCTION

Spectral domain optical coherence tomography (SD-OCT), being a noninvasive imaging modality, has begun to find vast use in the diagnosis and management of ocular diseases. Especially, it has advantages in monitoring the changes of retinal structure, such as the retinal nerve fiber layer (RNFL) and optic nerve cup. Layer segmentation methods designed

---

\*Corresponding author: E-mail: Xinjian.Chen@suda.edu.cn

for macular region of the retina have been extensively studied. In [1, 2], satisfactory results were obtained based on graph search method. In [3], a statistical models was utilized to segment the fovea-centered OCT images. Segmentation of the structures in ONH-centered OCT scans has also received considerable attention over the past few years. Antomy et al. [4] used graph-based approach to detect several intraretinal layers from ONH-centered OCT images. Vermeer et al. [5] segmented the retinal layers by pixel classification approach. However, due to the presence of irregularly shaped morphological features such as optic never head(ONH), segmentation is still a challenging problem. In this paper, we present an automated method that can segment the retinal layers in the ONH centered 3-D OCT volumes, which addresses the challenges posed by the presence of the large blood vessels and the optic disc. Fig.1(a) shows an original ONH-center OCT B-scan of a normal subject. Fig.1(b)shows a denoised and flattened image with segmentation result. Surface 1 to surface 7 from top to bottom define the 6 retinal layers. It is nerve fiber layer(NFL), ganglion cell layer and inner plexiform layer(GCL+IPL), inner nuclear layer and outer plexiform layer(INL+OPL), out nuclear layer and inner segment layer(ONL+ISL), connecting cilia ,outer segment layer and Verhoeff's membrane(CL+OSL+VM) and retinal pigment epithelium(RPE).

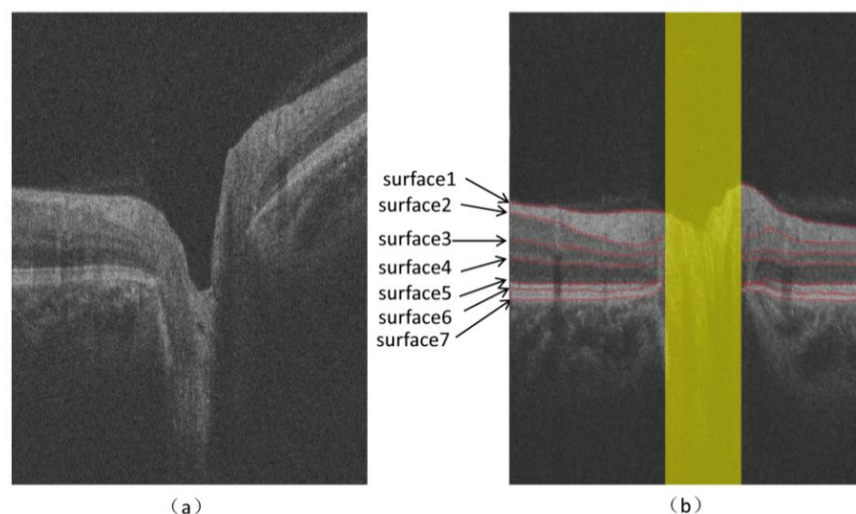


Fig.1 ONH centered OCT image of a normal eye and the 7 surfaces of the retinal layers. (a)original image (b) denoised and flattened image with segmentation result.

## 2. METHOD

The proposed framework consists of two main steps: preprocessing and layer segmentation(Fig.2).In the preprocessing step, a curvature anisotropic diffusion filter[6]is used to reduce the OCT speckle noise and four multi-scale OCT volumes are created by subsampling by a factor of 2 in the depth direction(z-axis). First, surface 1, 5 and 7 are detected and then the B-scans are flattened based on surface 5 (Fig.1).Subsequently, during layer segmentation, first, the AAM[7] is used to detect the surface 1, 2, 3, 4, 5, 6, 7 and the margin of optic disc. Secondly, a multi-resolution graph-search algorithm[1, 8] is applied for the further precise segmentation. Finally, the rim region of the optic disc is detected by shape prior model[9] on the projection image from surface 6 to surface 7. The rim region is masked out because the layers are hard to define in this region(Fig.4).

## 2.1 Preprocessing

The pre-processing part includes several steps. Firstly, gradient anisotropic diffusion filter is used to remove the speckles but maintaining the edge information in the image to the greatest extent. Despeckling can help to improve both the accuracy and the efficiency of the segmentation.

In addition, because SD-OCT is an in-vivo imaging technique, so the position of the scanner relative to the patient's pupil is not a fixed value and the eye movement was unavoidable, the volumetric data always has deformation. A flattening step is used to align the volumetric data, so that the 3-D context can be better utilized in the following processing. The flattening step is performed as follows. Using the multi-resolution surface detection method, we detect the most obvious surface 1 first. Using it as constraint, surface 7 is detected below the surface 1. Surface 5 is detected between the surface 1 and 7, and then smoothed by fitting a spline. The columns are shifted up or down such that surface 5 becomes flat. Finally, the rim region of the optic disc is detected by shape prior model[9] in the projection image from surface 6 to surface 7. The rim region is masked out because the layers are hard to define in this region(Fig.4).

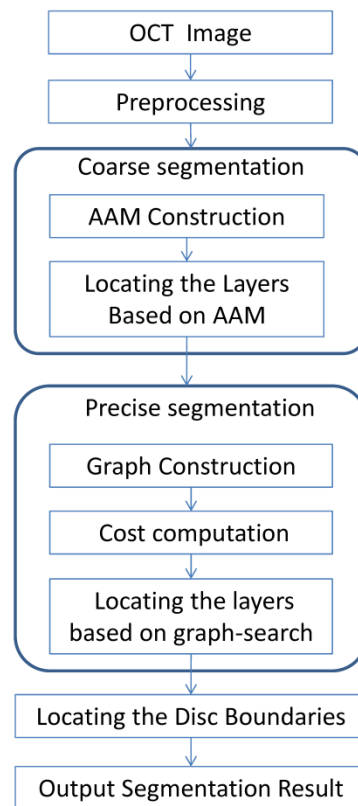


Fig.2 Flowchart of the proposed algorithm.

## 2.2 Coarse segmentation with Active Appearance Models

After the pre-processing stage, the ONH-centered retinal layers are coarsely segmented based on Active Appearance Models. The first step was training the statistical model on a set of annotated labels.

We manual annotated the seven surfaces in each B-scan of the training data. In practice, Surface 1 was labeled with 16 points. For surface 2 to surface 7, we labeled 6 points each in the two regions to the left and right of the rim region. Thus we have total 88 landmarks per image. Then the AAM is built based on these manual landmarks, which includes both shape and texture model,  $x$  and  $g$ , as follows:

$$\begin{aligned} x &= \bar{x} + Q_s s \\ g &= \bar{g} + Q_g t \end{aligned} \quad (1)$$

where  $\bar{x}$  is the mean shape,  $\bar{g}$  is the mean texture in a mean shaped patch,  $Q_s$  and  $Q_g$  are matrices describing the modes of variation derived from the training set,  $s$  and  $t$  is the shape and texture parameters, respectively.

The second step is locating the retinal surfaces. We adjust the model parameters to generate a synthetic image, which matches the target image as closely as possible. Thus the location of surfaces in the synthetic image provide a coarse delineation of the retinal surface on the target image.

### 2.3 Precise segmentation with Graph-Search

Based on the initial coarse segmentation result by the AAM, we can use 3D graph search algorithm which proposed by Li et al.[8] to get more accurate results.

In our proposed method, we used graph search for single surface detection to refine the surfaces detected by the AAM. Define the OCT volumetric image as a 3-D matrix  $I(x, y, z)$  of size  $X \times Y \times Z$ , and the boundaries of retinal layers are considered as terrainlike surfaces, defined by a function  $S(x, y)$ , where  $x \in \{0, \dots, X-1\}$ ,  $y \in \{0, \dots, Y-1\}$ , and  $S(x, y) \in \{0, \dots, Z-1\}$ . [1] Two feasibility constraints are used to find the surfaces. The first feasibility constraint is the location constraint, which defines the searching range of the surface. After coarse segmentation with AAM, the rough location of the surface has been found. Then the location constraint can be defined as a rang near the AAM result. Namely, the distance between the surface and AAM result is allowed to vary as a function of the  $(x, y)$  location, expressed as follows:

$$|S(x, y) - S_{AAM}(x, y)| \leq \delta(x, y) \quad (2)$$

The second feasibility constraint controls the smoothness of the surfaces[2]. Parameter  $\Delta_x$  defines the maximum change allowed in  $z$ -value between two voxels adjacent in the  $x$  direction, expressed as follows:

$$|S(x + 1, y) - S(x, y)| \leq \Delta_x \quad (3)$$

Parameter  $\Delta_y$  defines the maximum change allowed in  $z$ -value between two voxels adjacent in the  $y$  direction, expressed as follows:

$$|S(x, y + 1) - S(x, y)| \leq \Delta_y \quad (4)$$

During the layer segmentation, a weighted directed graph  $G = (v, e)$  is constructed, which is composed of a node set  $V$  and an arc set  $E$ . In the graph, the nodes  $v \in V$  corresponded to image voxels, and arcs  $\langle v_i, v_j \rangle \in E$  connected the nodes  $v_i, v_j$ . The weight  $w(x, y, z)$  of the node  $v \in V$  is derived from the cost function which can be expressed as some measure (e.g., gradients) of the corresponding voxels belonging to the surface. The weight of each node is computed as follows:

$$w(x, y, z) = \begin{cases} c(x, y, z), & \text{if } z = 0 \\ c(x, y, z) - c(x, y, z - 1) & \text{otherwise} \end{cases} \quad (5)$$

By finding an optimal closed set in a vertex-weighted graph, the optimal surface is found. Compared with the traditional graph search, by adding the location constraint obtained by AAM, the proposed approach is able to segment the intraretinal surfaces more precisely.

### 2.4 Detect the border of the ONH

In the ONH area of the retinal, because of the blood vessels and nervus opticus converge in the neural canal, retinal tissue was disconnected in the region. The surfaces become inexistence in the neural canal. So it is hard to be delineated. Thus, the neural canal must be avoided while tracing and validating the segmentation results.

We used an active contour algorithm that using prior shapes[9] to detect the optic disk border. The method begins with the creation of a projection image from surface 6 to surface7. Optic disc region was detected with AAM method can be used as prior shapes for further improve segmentation result of disk border.

The energy of the contour depends on the image gradient as well as the prior shape. The model provides the segmentation and the transformation that maps the segmented contour to the prior shape. The active contour is able to find boundaries that are similar in shape to the prior when the energy functional of the contour has the minimum. Fig.4 shows an example which the rim region is masked out, because of the layers are hard to define in this region.

## 3. RESULTS

The proposed method was applied to 11 ONH centered SD-OCT images from 11 normal subjects(6 used as training set, 5 used as testing set). Each data were acquired using Topcon 3D-OCT 2000 (Topcon Corporation, Tokyo, Japan) representing a  $6\text{mm} \times 6\text{mm} \times 2.3\text{mm}$  region which contained  $512 \times 128 \times 885$  voxels. To evaluate the layer segmentation results, the algorithm was tested against the ground truth which was defined as the average of two independent manual tracings by retinal specialists. Because manual segmentation is time-consuming, only 8 out of 128 B-scans (evenly spaced) were labeled for each 3-D OCT volume.

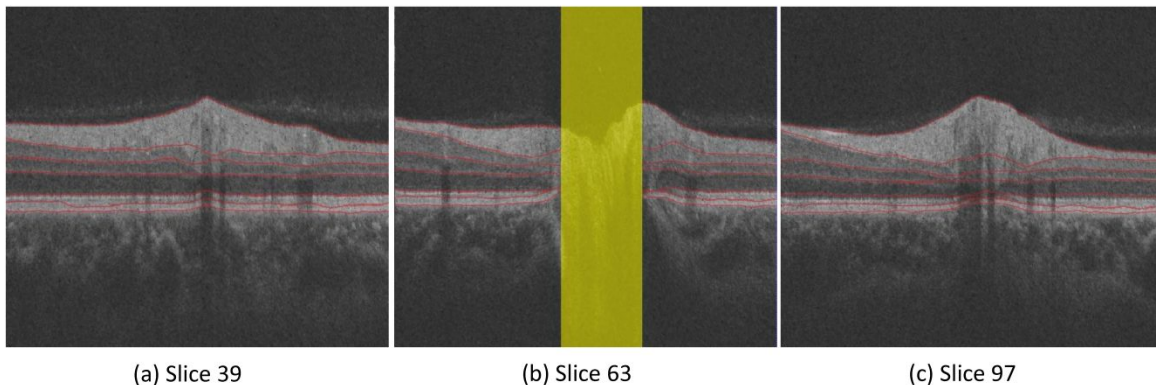


Fig.3 Segmentation results on some B-scans in OCT image from a normal subject.

Fig.3 shows an example of the intraretinal layers segmentation results on 3 B-scans. To prove the significance of using AAM to constrain graph search, we compare the proposed method with conventional graph search (GS) and inter-observer variability. The mean and standard deviation of unsigned border positioning errors were computed for all manually traced B-scans from the ONH centered dataset, and are shown in Table 1. The overall mean border positioning error for layer segmentation was found to be  $7.09 \pm 6.18 \mu\text{m}$  for our proposed method,  $8.03 \pm 10.47 \mu\text{m}$  for the traditional graph search method and  $6.35 \pm 6.93 \mu\text{m}$  for mean inter-observer variability.

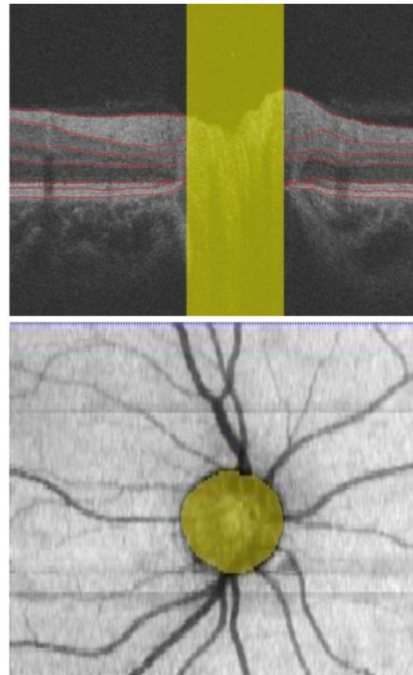


Fig.4 A central B-scan of a dataset with yellow indicating the rim region.

Table 1. Summary of unsigned border positioning errors\* for all labeled B-Scan

Surface	Algo. vs. GT	Graph search vs GT	Obs.1 vs. Obs.2
1	4.76±3.59	6.65±15.72	5.47±7.33
2	7.63±6.63	10.97±13.31	8.67±7.50
3	8.53±8.89	9.09±8.67	5.09±7.75
4	7.67±6.58	7.72±7.53	7.78±9.50
5	6.04±4.72	6.21±4.07	5.58±4.34
6	6.85±5.28	7.16±5.79	6.01±4.75
7	8.25±5.27	8.80±10.31	6.19±4.91
overall	7.09±6.18	8.03±10.47	6.36±6.93

\*Mean ± SD in  $\mu\text{m}$ ,  $2.6 \mu\text{m} = 1\text{pixel}$

#### 4. DISCUSSION AND CONCLUSION

In this paper, we propose an automated 3-D framework for retinal layers segmentation in ONH centered 3-D OCT images. This method efficiently combines the AAM and graph search methods to overcome the difficulties for segmenting the complex structure of ONH. The global shape-constrained GS-AAM method addresses the challenges posed by the presence of the neural canal, large blood vessels and the optic disc. The proposed framework consists of two main steps: (1) Coarse segmentation based on AAM algorithm. (2) precise segmentation based on GS-AAM algorithm. The preliminary results show the feasibility and efficiency of the proposed method.

There are a number of possible improvements to our work. First, it is only tested on normal subjects. We will evaluate this algorithm on the glaucoma subjects in future work. Second, more layers can be segmented. Last, because multi-modality imaging has become a standard method in clinical pathological analysis, in the future, we can use fundus images to aid detection of the optic disc and cup margin and try to produce more accurate segmentation results.

#### 5. ACKNOWLEDGMENTS

This work was supported in part by the National Basic Research Program of China (973 Program) under Grant 2014CB748600, and in part by the National Natural Science Foundation of China (NSFC) under Grant 61401294, 81401472, 81371629, 6140293, and in part by Natural Science Foundation of the Jiangsu Province under Grant BK20140052, and in part by Natural Science Foundation of the Jiangsu Higher Education of China under Grant 14KJB510032.

#### REFERENCE

- [1] Garvin M K, Abramoff M D, Wu X, et al. Automated 3-D Intraretinal Layer Segmentation of Macular Spectral-Domain Optical Coherence Tomography Images[J]. IEEE Transactions on Medical Imaging, 2009, 28(9):1436-1447.
- [2] Shi F, Chen X, Zhao H, et al. Automated 3-D retinal layer segmentation of macular optical coherence tomography images with serous pigment epithelial detachments.[J]. IEEE transactions on medical imaging, 2015, 34(2):441-52.
- [3] Kajić V, Považay B, Hermann B, et al. Robust segmentation of intraretinal layers in the normal human fovea using a novel statistical model based on texture and shape analysis[J]. Optics Express, 2010, 18(14):14730-44.
- [4] Antony B J, Lee K, Sonkova P, et al. Automated 3D segmentation of intraretinal layers from optic nerve head optical coherence tomography images[J]. Proceedings of SPIE - The International Society for Optical Engineering, 2010, 7626(1):666-673.
- [5] Yin F, Liu J, Ong S H, et al. Model-based optic nerve head segmentation on retinal fundus images.[C]// International Conference of the IEEE Engineering in Medicine & Biology Society. Conf Proc IEEE Eng Med Biol Soc, 2011:2626-9.
- [6] Perona P, Malik J. Scale-space and edge detection using anisotropic diffusion[J]. IEEE Transactions on Pattern Analysis & Machine Intelligence, 1990, 12(7):629-639.
- [7] Chen X, Udupa J K, Bagci U, et al. Medical Image Segmentation by Combining Graph Cuts and Oriented Active Appearance Models[J]. IEEE Transactions on Image Processing A Publication of the IEEE Signal Processing Society, 2012, 21(4):2035-2046.

- [8] Li K, Wu X, Chen D Z, et al. Optimal Surface Segmentation in Volumetric Images-A Graph-Theoretic Approach[J]. IEEE Transactions on Pattern Analysis & Machine Intelligence, 2006, 28(1):119-34.
- [9] Chen Y, Tagare H D, Thiruvankadam S, et al. Using Prior Shapes in Geometric Active Contours in a Variational Framework[J]. International Journal of Computer Vision, 2002, 50(3):315-328.